JOURNAL OF GUIDANCE, CONTROL, AND DYNAMICS
Vol. 25, No. 2, March–April 2002

Characteristics of Time-Optimal Commands for Flexible Structures with Limited Fuel Usage

Mark A. Lau and Lucy Y. Pao
University of Colorado, Boulder, Colorado 80309-0425

A mathematical justification is provided for time-optimal and fuel-efficient controllers based on analysis of the switching function for the control. That some symmetry properties of time-optimal commands, which are known to hold for undamped flexible structures, remain valid in the presence of fuel constraints is demonstrated. These properties, however, do not hold for robust time-optimal commands with specified fuel.

Introduction

CONTROL of flexible structures has been extensively investigated by many researchers in the last decade because a growing number of applications involve very lightweight structures.[1,2] In general, systems are required to meet certain performance criteria. For instance, one possible criterion is the minimum time required for completing a transfer of the system from one state to another state. This constitutes a typical time-optimal problem that pertains to the realm of optimal control theory. The foundations of the theory are well established by now and an introduction to this field may be found in Ref. 3.

Control strategies based exclusively on rigid-body dynamics may not be suitable for adequate performance if the effects of elastic modes are appreciable. Consideration of these effects becomes an integral part for the understanding of system behavior and control design. Early work on time-optimal control of flexible structures[4–6] shows that the resulting optimal bang–bang commands satisfy certain symmetry properties when the structures have no damping. Robust time-optimal designs obtained from additional derivative constraints[7,8] can significantly improve the insensitivity to parameter variations. The effects of damping on time-optimal commands[9,10] have also been recently investigated.

Incorporating fuel expenditure as a design factor alters the array of possibilities for feasible controllers. A modified performance criterion[11] can be used to balance speed of transfer and fuel consumption by simply adjusting a design parameter. Fuel-efficient shaped command profiles[12] and specified fuel usage[13] can significantly save fuel compared to time-optimal commands without fuel limits.

This paper presents a mathematical justification for the occurrence of the command profiles assumed in Refs. 12 and 13 based on Pontryagin's minimum principle.[3] In contrast, in this work, the different command profiles that arise in the time-optimal with specified fuel problem are derived from the analysis of the switching function and not by insights gained from an input shaping interpretation.[12,13] The paper is organized as follows. We first formulate the time-optimal problem with specified fuel for a certain class of systems, and we then apply this theory to the analysis of flexible structures. Subsequently, we extend some known properties of the optimal commands for undamped flexible structures in the presence of fuel constraints. Robustness issues, a procedure for designing robust time-optimal commands with specified fuel and the nonexistence of symmetry in these robust commands are also discussed. Finally, we present concluding remarks.

Mark A. Lau received his B.S. in Engineering Sciences and diploma in Industrial Engineering from the University of Piura, Peru, in 1988 and 1991, respectively. He attended the University of Colorado at Boulder and earned his M.S. and Ph.D. in Electrical Engineering in 1997 and 2000, respectively. He was the winner of the Best Student Paper Award at the 2001 American Control Conference. His research interests are in the control of flexible structures, optimization, process control, microelectromechanical systems, and nanotechnology. E-mail: mark.lau@colorado.edu.

Lucy Y. Pao received her B.S., M.S., and Ph.D. degrees in Electrical Engineering from Stanford University in 1987, 1988, and 1992, respectively. From 1991–1993, she worked at the MITRE Corporation, and from 1993–1995, she was an Assistant Professor in the Electrical Engineering and Computer Science Department at Northwestern University. Since 1995, she has been with the Electrical and Computer Engineering Department at the University of Colorado at Boulder, where she is now an Associate Professor. She is spending 2001–2002 as a Visiting Professor at both Harvard University and the Massachusetts Institute of Technology in Cambridge, Massachusetts. She is the recipient of the 1996 International Federation of Automatic Control (IFAC) World Congress Young Author Prize, a National Science Foundation Early Faculty CAREER Development Award (1996–2001), and an Office of Naval Research Young Investigator Award (1997–2000). She has also been on the Organizing Committee for the International Symposium on Motion and Vibration Control (1999) and on the International Program Committee for the Japan/U.S.A./Vietnam Workshop on Research and Education in Systems, Computation, and Control Engineering (2000). She is on the International Program Committee for the IFAC Conference on Mechatronic Systems (2002), and she will be the Vice Chair for Invited Sessions for the 2003 American Control Conference and the Program Chair for the 2004 American Control Conference. Her research interests are in control of flexible structures, multisensor data fusion, and haptic and visual/haptic interfaces. E-mail: pao@colorado.edu.

Received 25 January 2001; revision received 14 June 2001; accepted for publication 19 July 2001.

Problem Formulation

In this section, we review the formulation of the time-optimal control problem subject to fuel limitations.[3] Let us denote the state of an nth-order system at time t by the n vector $\boldsymbol{x}(t)$ and assume that the state equations of the system are of the form

$$\dot{\boldsymbol{x}}(t) = \boldsymbol{a}[\boldsymbol{x}(t), t] + \boldsymbol{B}[\boldsymbol{x}(t), t]\boldsymbol{u}(t) \tag{1}$$

where $\boldsymbol{a}$ is an n-vector function of the state and time, $\boldsymbol{B}$ is an $n \times m$ matrix that may be explicitly dependent on the state and time, and $\boldsymbol{u}$ is an m-control vector. The controls $\boldsymbol{u}$ are to drive the system from some initial state $\boldsymbol{x}_0$ to the origin in minimum time. That is, the performance measure to be minimized is

$$J(\boldsymbol{u}) = \int_{t_0}^{t_f} \mathrm{d}t = t_f - t_0 \tag{2}$$

and the admissible controls are to satisfy the saturation constraint

$$|u_i(t)| \le U_{\max_i}, \qquad i = 1, \dots, m \tag{3}$$

and fuel constraint

$$\int_{t_0}^{t_f} \left[\sum_{i=1}^{m} |u_i(t)|\right] \mathrm{d}t \le S \tag{4}$$

where S represents the fuel available. If S is so large that the time-optimal control without fuel constraint does not cause all of the fuel to be consumed, then there is no fuel limitation constraint required. If the time-optimal control without fuel limitation requires an amount of fuel that exceeds S, then the fuel limitation must be included, and the time-optimal control subject to fuel limitation is such that all of the fuel is consumed. In this case, the inequality in Eq. (4) can be replaced with the equality constraint (specified fuel constraint),

$$\int_{t_0}^{t_f} \left[\sum_{i=1}^{m} |u_i(t)|\right] \mathrm{d}t = S \tag{5}$$

We wish to formulate the stated problem as a canonical time-optimal problem using Pontryagin's minimum principle.[3] To that end, we define a new variable

$$z(t) = \int_{t_0}^{t} \left[\sum_{i=1}^{m} |u_i(\tau)|\right] \mathrm{d}\tau - S \tag{6}$$

and, therefore,

$$\dot{z}(t) = \sum_{i=1}^{m} |u_i(t)| \tag{7}$$

where the boundary conditions for $z(t)$ are $z(t_0) = -S$ and $z(t_f) = 0$, respectively. Equation (7) can be appended to the original system (1), and then we have an augmented system in the canonical form of a time-optimal problem because the only constraint remaining is given by Eq. (3).

Let us call $\boldsymbol{p}(t)$ and $p_z(t)$ the Lagrange multipliers of the original system (1) and the augmented state $z(t)$, respectively. Then, the Hamiltonian is

$$\begin{aligned}\mathcal{H}[\boldsymbol{x}(t), \boldsymbol{u}(t), \boldsymbol{p}(t), p_z(t), t] &= 1 + \boldsymbol{p}^T(t)\{\boldsymbol{a}[\boldsymbol{x}(t), t] \\ &\quad + \boldsymbol{B}[\boldsymbol{x}(t), t]\boldsymbol{u}(t)\} + p_z(t)\left[\sum_{i=1}^{m} |u_i(t)|\right]\end{aligned} \tag{8}$$

That $p_z(t)$ is a constant follows readily because the Hamiltonian does not depend explicitly on z. Thus, in the following we will just write p_z. The Hamiltonian for the augmented system is identical to the one defined for a fuel/time-optimal problem where $p_z > 0$ represents the relative weight of the fuel consumed in the cost functional.[11,13]

From Pontryagin's minimum principle,

$$\begin{aligned}&1 + \boldsymbol{p}^{*T}(t)\{\boldsymbol{a}[\boldsymbol{x}^*(t), t] + \boldsymbol{B}[\boldsymbol{x}^*(t), t]\boldsymbol{u}^*(t)\} + p_z^*\left[\sum_{i=1}^{m} \left|u_i^*(t)\right|\right] \\ &\le 1 + \boldsymbol{p}^{*T}(t)\{\boldsymbol{a}[\boldsymbol{x}^*(t), t] + \boldsymbol{B}[\boldsymbol{x}^*(t), t]\boldsymbol{u}(t)\} \\ &\quad + p_z^*\left[\sum_{i=1}^{m} |u_i(t)|\right]\end{aligned} \tag{9}$$

where the asterisk denotes optimal quantities for all admissible $\boldsymbol{u}(t)$ and for all $t \in [t_0, t_f]$. The preceding equation implies

$$\begin{aligned}&\boldsymbol{p}^{*T}(t)\boldsymbol{B}[\boldsymbol{x}^*(t), t]\boldsymbol{u}^*(t) + p_z^*\left[\sum_{i=1}^{m} \left|u_i^*(t)\right|\right] \\ &\le \boldsymbol{p}^{*T}(t)\boldsymbol{B}[\boldsymbol{x}^*(t), t]\boldsymbol{u}(t) + p_z^*\left[\sum_{i=1}^{m} |u_i(t)|\right]\end{aligned} \tag{10}$$

If we express the matrix $\boldsymbol{B}$ in terms of its columns $\boldsymbol{b}_i[\boldsymbol{x}^*(t), t]$, $i = 1, \dots, m$, then the coefficient of the ith control component $u_i(t)$ is $\boldsymbol{p}^{*T}(t)\boldsymbol{b}_i[\boldsymbol{x}^*(t), t]$, and we can rewrite Eq. (10) as

$$\begin{aligned}&\sum_{i=1}^{m} \left\{\boldsymbol{p}^{*T}(t)\boldsymbol{b}_i[\boldsymbol{x}^*(t), t]u_i^*(t) + p_z^*\left|u_i^*(t)\right|\right\} \\ &\le \sum_{i=1}^{m} \left\{\boldsymbol{p}^{*T}(t)\boldsymbol{b}_i[\boldsymbol{x}^*(t), t]u_i(t) + p_z^*|u_i(t)|\right\}\end{aligned} \tag{11}$$

If the control components are independent of one another, we then must minimize

$$\boldsymbol{p}^{*T}(t)\boldsymbol{b}_i[\boldsymbol{x}^*(t), t]u_i(t) + p_z^*|u_i(t)| \tag{12}$$

and from the definition of absolute value, we have

$$\begin{aligned}&\boldsymbol{p}^{*T}(t)\boldsymbol{b}_i[\boldsymbol{x}^*(t), t]u_i(t) + p_z^*|u_i(t)| \\ &= \begin{cases}\left\{\boldsymbol{p}^{*T}(t)\boldsymbol{b}_i[\boldsymbol{x}^*(t), t] + p_z^*\right\}u_i(t), & u_i(t) \ge 0 \\ \left\{\boldsymbol{p}^{*T}(t)\boldsymbol{b}_i[\boldsymbol{x}^*(t), t] - p_z^*\right\}u_i(t), & u_i(t) \le 0\end{cases}\end{aligned} \tag{13}$$

Hence, the optimal control is given by

$$u_i^*(t) = \begin{cases} U_{\max_i}, & \text{for} \quad \boldsymbol{p}^{*T}(t)\boldsymbol{b}_i[\boldsymbol{x}^*(t), t] < -p_z \\ 0, & \text{for} \quad -p_z < \boldsymbol{p}^{*T}(t)\boldsymbol{b}_i[\boldsymbol{x}^*(t), t] < p_z \\ -U_{\max_i}, & \text{for} \quad p_z < \boldsymbol{p}^{*T}(t)\boldsymbol{b}_i[\boldsymbol{x}^*(t), t] \\ \text{an undetermined nonnegative value} & \\ \quad \text{if} \quad \boldsymbol{p}^{*T}(t)\boldsymbol{b}_i[\boldsymbol{x}^*(t), t] = -p_z & \\ \text{an undetermined nonpositive value} & \\ \quad \text{if} \quad \boldsymbol{p}^{*T}(t)\boldsymbol{b}_i[\boldsymbol{x}^*(t), t] = p_z & \end{cases} \tag{14}$$

similar to the bang–off–bang patterns obtained in fuel-optimal problems. In a fuel-optimal problem, $p_z = \pm 1$, whereas in the time-optimal with fuel limitation problem, p_z is any scalar.

Flexible Structures

Consider a one-bending-mode flexible structure modeled by

$$\dot{\boldsymbol{x}}(t) = \boldsymbol{A}\boldsymbol{x}(t) + \boldsymbol{b}u(t) \tag{15}$$

where

$$\boldsymbol{A} = \begin{bmatrix} 0 & 1 & 0 & 0 \\ 0 & 0 & 0 & 0 \\ 0 & 0 & 0 & 1 \\ 0 & 0 & -\omega^2 & -2\zeta\omega \end{bmatrix}, \qquad \boldsymbol{b} = \begin{bmatrix} 0 \\ 1 \\ 0 \\ b_1 \end{bmatrix}$$

$$\boldsymbol{x} = \begin{bmatrix} x_1 \\ x_2 \\ x_3 \\ x_4 \end{bmatrix} = \begin{bmatrix} \text{rigid body position} \\ \text{rigid body velocity} \\ \text{modal position} \\ \text{modal velocity} \end{bmatrix}$$

where ω is the structural frequency, ζ is the damping ratio of the flexible mode, and $b_1 \neq 0$.

The time-optimal control for rest-to-rest motion is to find the scalar control $u(t)$ subject to the constraints (actuator limits)

$$|u(t)| \leq U_0$$

and (specified fuel)

$$\int_0^{t_f} |u(t)|\,\mathrm{d}t = S$$

so that the motion of the system is transferred from an initial rest state $\boldsymbol{x}(0) = [x_{10}\ \ 0\ \ 0\ \ 0]^T$ to the origin $\boldsymbol{x}(t_f) = [0\ \ 0\ \ 0\ \ 0]^T$ while the maneuver time t_f is minimized.

We form the Hamiltonian of the augmented system,

$$\mathcal{H}(\boldsymbol{x}, u, \boldsymbol{p}, p_z) = 1 + p_1 x_2 + p_2 u + p_3 x_4 + p_4\big(-\omega^2 x_3 - 2\zeta\omega x_4 + b_1 u\big) + p_z|u|$$

and obtain the costate equations

$$p_1(t) = p_{10}$$

$$p_2(t) = -p_{10}t + p_{20}$$

$$p_3(t) = \frac{\exp(\zeta\omega t)}{\omega_d}\big\{p_{30}[\omega_d\cos(\omega_d t) - \zeta\omega\sin(\omega_d t)] + p_{40}\omega^2\sin(\omega_d t)\big\}$$

$$p_4(t) = \frac{\exp(\zeta\omega t)}{\omega_d}\{-p_{30}\sin(\omega_d t) + p_{40}[\omega_d\cos(\omega_d t) + \zeta\omega\sin(\omega_d t)]\}$$

$$p_z(t) = p_z$$

where $\omega_d = \omega\sqrt{(1-\zeta^2)}(0 \leq \zeta < 1)$, for some constants p_{10}, p_{20}, p_{30}, p_{40}, and p_z. Therefore, the switching function has the form

$$\boldsymbol{p}^T(t)\boldsymbol{b} = c_1 + c_2 t + \exp(\zeta\omega t)[c_3\sin(\omega_d t) + c_4\cos(\omega_d t)] \tag{16}$$

where

$$c_1 = p_{20}, \qquad c_2 = -p_{10}$$

$$c_3 = b_1(-p_{30} + \zeta\omega p_{40})/\omega_d, \qquad c_4 = b_1 p_{40}$$

The switching function given in Eq. (16) is a modulated wave contained in an exponential envelope, that is,

$$\exp(\zeta\omega t)[c_3\sin(\omega_d t) + c_4\cos(\omega_d t)]$$

and symmetric about the line $c_1 + c_2 t$. The intersection of the horizontal lines $p_z(t) = p_z (p_z > 0)$ and $-p_z$ with the curve given by Eq. (16) indicates multiple crossings over a finite interval of time. Examination of the orientation of the envelope and the crossings of the wave with the horizontal lines show that, of all of the possible optimal command profiles, the ones that lead to optimal controls $u^*(t)$ exhibit regular patterns and have either one of two forms, which we shall denote case I and case II (as shown in Fig. 1).

Case I

Here

$$u^*(t) = \alpha U_0 \sum_{k=0}^{m}\big[(-1)^k\mathbf{1}(t - t_{2k}) + (-1)^{k+1}\mathbf{1}(t - t_{2k+1})\big] \tag{17}$$

where m is the number of sign reversals of the control, that is, from $+U_0$ to $-U_0$ and vice versa, ignoring the off periods, α is the initial sign of the control, and $\mathbf{1}(t - t_i)$ denotes a unit step input applied at time t_i. The control given by Eq. (17) suggests that the optimal control with fuel constraint introduces off periods at the locations where a switch normally occurs in a bang–bang command without fuel constraint.

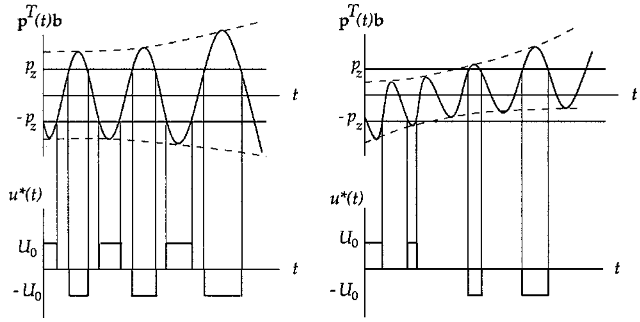

Fig. 1 Typical control profile patterns.

Solving Eq. (15) with the control in Eq. (17), we get the state equations for $t \geq t_f$,

$$x_1(t) = x_{10} + x_{20}t + \frac{\alpha U_0}{2}\left\{\sum_{k=0}^{m}\big[(-1)^k(t - t_{2k})^2 + (-1)^{k+1}(t - t_{2k+1})^2\big]\right\}$$

$$x_2(t) = x_{20} + \alpha U_0\left\{\sum_{k=0}^{m}\big[(-1)^k(t - t_{2k}) + (-1)^{k+1}(t - t_{2k+1})\big]\right\}$$

$$\begin{aligned}x_3(t) = {}& \frac{\exp(-\zeta\omega t)}{\omega_d}\{x_{30}[\omega_d\cos(\omega_d t) + \zeta\omega\sin(\omega_d t)] + x_{40}\sin(\omega_d t)\} + \frac{\alpha b_1 U_0}{\omega^2}\left\{\sum_{k=0}^{m}\Bigg[(-1)^k\right.\\ &\times\left(1 - \frac{\exp[-\zeta\omega(t - t_{2k})]}{\omega_d}\{\omega_d\cos[\omega_d(t - t_{2k})] + \zeta\omega\sin[\omega_d(t - t_{2k})]\}\right) + (-1)^{k+1}\\ &\times\left.\left(1 - \frac{\exp[-\zeta\omega(t - t_{2k+1})]}{\omega_d}\{\omega_d\cos[\omega_d(t - t_{2k+1})] + \zeta\omega\sin[\omega_d(t - t_{2k+1})]\}\right)\Bigg]\right\}\end{aligned}$$

$$\begin{aligned}x_4(t) = {}& \frac{\exp(-\zeta\omega t)}{\omega_d}\big\{-x_{30}\omega^2\sin(\omega_d t) + x_{40}[\omega_d\cos(\omega_d t) - \zeta\omega\sin(\omega_d t)]\big\} + \frac{\alpha b_1 U_0}{\omega_d}\left(\sum_{k=0}^{m}\big\{(-1)^k\exp[-\zeta\omega(t - t_{2k})]\right.\\ &\times\sin[\omega_d(t - t_{2k})] + (-1)^{k+1}\exp[-\zeta\omega(t - t_{2k+1})]\\ &\times\left.\sin[\omega_d(t - t_{2k+1})]\big\}\right)\end{aligned}$$

$$z(t) = U_0\sum_{k=0}^{2m}(-1)^k t_{k+1} - S \tag{18}$$

where we denote $t_f = t_{2m+1}$ and assume, without loss of generality, that $t_0 = 0$.

For rest-to-rest motion we set $\boldsymbol{x}(0) = [-L\ \ 0\ \ 0\ \ 0]^T$ and $\boldsymbol{x}(t_f) = [0\ \ 0\ \ 0\ \ 0]^T$ along with $z(0) = -S$ and $z(t_f) = 0$ in Eq. (18) to get

$$x_1(t_f) = -L + \frac{\alpha U_0}{2}\left\{\sum_{k=0}^{m}\left[(-1)^k(t_f - t_{2k})^2 + (-1)^{k+1}(t_f - t_{2k+1})^2\right]\right\} = 0$$

$$x_2(t_f) = \alpha U_0\left\{\sum_{k=0}^{m}\left[(-1)^k(t_f - t_{2k}) + (-1)^{k+1}(t_f - t_{2k+1})\right]\right\} = 0$$

$$x_3(t_f) = \frac{\alpha b_1 U_0}{\omega^2}\left\{\sum_{k=0}^{m}\left[(-1)^k\left(1 - \frac{\exp[-\zeta\omega(t_f - t_{2k})]}{\omega_d} \times \{\omega_d\cos[\omega_d(t_f - t_{2k})] + \zeta\omega\sin[\omega_d(t_f - t_{2k})]\}\right) + (-1)^{k+1}\left(1 - \frac{\exp[-\zeta\omega(t_f - t_{2k+1})]}{\omega_d} \times \{\omega_d\cos[\omega_d(t_f - t_{2k+1})] + \zeta\omega\sin[\omega_d(t_f - t_{2k+1})]\}\right)\right]\right\} = 0$$

$$x_4(t_f) = \frac{\alpha b_1 U_0}{\omega_d}\left(\sum_{k=0}^{m}\left\{(-1)^k\exp[-\zeta\omega(t_f - t_{2k})] \times \sin[\omega_d(t_f - t_{2k})] + (-1)^{k+1}\exp[-\zeta\omega(t_f - t_{2k+1})] \times \sin[\omega_d(t_f - t_{2k+1})]\right\}\right) = 0$$

$$z(t_f) = U_0\sum_{k=0}^{2m}(-1)^k t_{k+1} - S = 0 \tag{19}$$

which can be further simplified to obtain the following constraints on the switching times:

$$\sum_{k=0}^{m}\left[(-1)^k t_{2k}^2 + (-1)^{k+1}t_{2k+1}^2\right] = \frac{2L}{\alpha U_0}$$

$$\sum_{k=0}^{m}\left[(-1)^{k+1}t_{2k} + (-1)^k t_{2k+1}\right] = 0$$

$$\sum_{k=0}^{m}\left[(-1)^k\exp(\zeta\omega t_{2k})\cos(\omega_d t_{2k}) + (-1)^{k+1}\exp(\zeta\omega t_{2k+1})\cos(\omega_d t_{2k+1})\right] = 0$$

$$\sum_{k=0}^{m}\left[(-1)^k\exp(\zeta\omega t_{2k})\sin(\omega_d t_{2k}) + (-1)^{k+1}\exp(\zeta\omega t_{2k+1})\sin(\omega_d t_{2k+1})\right] = 0$$

$$U_0\sum_{k=0}^{2m}(-1)^k t_{k+1} = S \tag{20}$$

In summary, we have formulated the original optimal control problem as a parameter optimization problem. That is, we want to minimize t_f (or t_{2m+1}) subject to the constraints in Eq. (20).

Case II

Here

$$u^*(t) = \alpha U_0\left[\sum_{k=0}^{2m-1}(-1)^k\mathbf{1}(t - t_k) + \sum_{k=2m}^{2m+2n-1}(-1)^{k+1}\mathbf{1}(t - t_k)\right] \tag{21}$$

where the control given by Eq. (21) consists of a sequence of m pulses of one sign followed by a sequence of n pulses of the opposite sign.

Solving Eq. (15) with the control in Eq. (21), we get the state equations for $t \geq t_f$,

$$x_1(t) = x_{10} + x_{20}t + \frac{\alpha U_0}{2}\left\{\sum_{k=0}^{2m-1}(-1)^k(t - t_k)^2 + \sum_{k=2m}^{2m+2n-1}(-1)^{k+1}(t - t_k)^2\right\}$$

$$x_2(t) = x_{20} + \alpha U_0\left\{\sum_{k=0}^{2m-1}(-1)^k(t - t_k) + \sum_{k=2m}^{2m+2n-1}(-1)^{k+1}(t - t_k)\right\}$$

$$x_3(t) = \frac{\exp(-\zeta\omega t)}{\omega_d}\{x_{30}[\omega_d\cos(\omega_d t) + \zeta\omega\sin(\omega_d t)] + x_{40}\sin(\omega_d t)\} + \frac{\alpha b_1 U_0}{\omega^2}\left[\sum_{k=0}^{2m-1}(-1)^k \times \left(1 - \frac{\exp[-\zeta\omega(t - t_k)]}{\omega_d}\{\omega_d\cos[\omega_d(t - t_k)] + \zeta\omega\sin[\omega_d(t - t_k)]\}\right) + \sum_{k=2m}^{2m+2n-1}(-1)^{k+1} \times \left(1 - \frac{\exp[-\zeta\omega(t - t_k)]}{\omega_d}\{\omega_d\cos[\omega_d(t - t_k)] + \zeta\omega\sin[\omega_d(t - t_k)]\}\right)\right]$$

$$x_4(t) = \frac{\exp(-\zeta\omega t)}{\omega_d}\left\{-x_{30}\omega^2\sin(\omega_d t) + x_{40}[\omega_d\cos(\omega_d t) - \zeta\omega\sin(\omega_d t)]\right\} + \frac{\alpha b_1 U_0}{\omega_d}\left\{\sum_{k=0}^{2m-1}(-1)^k\exp[-\zeta\omega(t - t_k)] \times \sin[\omega_d(t - t_k)] + \sum_{k=2m}^{2m+2n-1}(-1)^{k+1}\exp[-\zeta\omega(t - t_k)] \times \sin[\omega_d(t - t_k)]\right\}$$

$$z(t) = U_0\sum_{k=0}^{2m+2n-2}(-1)^k t_{k+1} - S \tag{22}$$

where we denote $t_f = t_{2m+2n-1}$ and again assume that $t_0 = 0$.

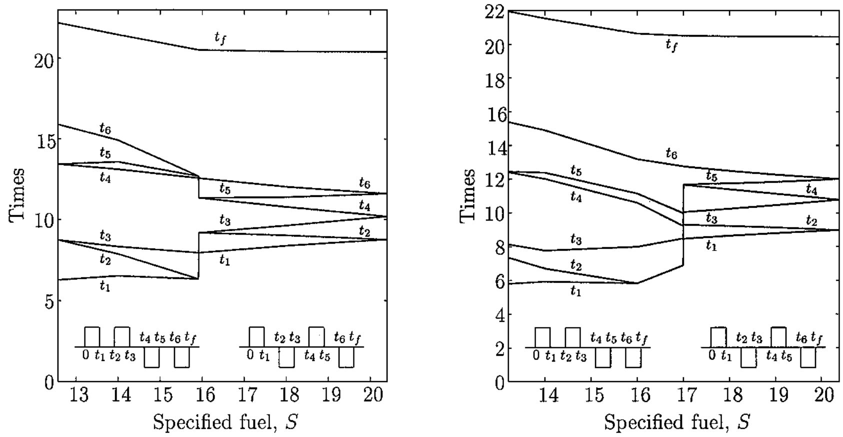

a) $\omega_{\text{model}} = 1$, $\zeta_{\text{model}} = 0$, and $L = 10$

b) $\omega_{\text{model}} = 1$, $\zeta_{\text{model}} = 0.05$, and $L = 100$

Fig. 2 Switching and maneuver times as a function of specified fuel.

For rest-to-rest motion as defined in case I, we obtain

$$x_1(t_f) = -L + \frac{\alpha U_0}{2}\left\{\sum_{k=0}^{2m-1}(-1)^k(t_f - t_k)^2 + \sum_{k=2m}^{2m+2n-1}(-1)^{k+1}(t_f - t_k)^2\right\} = 0$$

$$x_2(t_f) = \alpha U_0\left\{\sum_{k=0}^{2m-1}(-1)^k(t_f - t_k) + \sum_{k=2m}^{2m+2n-1}(-1)^{k+1}(t_f - t_k)\right\} = 0$$

$$x_3(t_f) = \frac{\alpha b_1 U_0}{\omega^2}\left\{\sum_{k=0}^{2m-1}(-1)^k\left(1 - \frac{\exp[-\zeta\omega(t_f - t_k)]}{\omega_d} \times \{\omega_d\cos[\omega_d(t_f - t_k)] + \zeta\omega\sin[\omega_d(t_f - t_k)]\}\right) + \sum_{k=2m}^{2m+2n-1}(-1)^{k+1}\left(1 - \frac{\exp[-\zeta\omega(t_f - t_k)]}{\omega_d} \times \{\omega_d\cos[\omega_d(t_f - t_k)] + \zeta\omega\sin[\omega_d(t_f - t_k)]\}\right)\right\} = 0$$

$$x_4(t_f) = \frac{\alpha b_1 U_0}{\omega_d}\left\{\sum_{k=0}^{2m-1}(-1)^k\exp[-\zeta\omega(t_f - t_k)]\sin[\omega_d(t_f - t_k)] + \sum_{k=2m}^{2m+2n-1}(-1)^{k+1}\exp[-\zeta\omega(t_f - t_k)]\sin[\omega_d(t_f - t_k)]\right\} = 0$$

$$z(t_f) = U_0\sum_{k=0}^{2m+2n-2}(-1)^k t_{k+1} - S = 0 \tag{23}$$

Again, simplifying the expressions, we can reformulate the problem as the following constrained optimization problem: Minimize t_f subject to

$$\sum_{k=0}^{2m-1}(-1)^k t_k^2 + \sum_{k=2m}^{2m+2n-1}(-1)^{k+1}t_k^2 = \frac{2L}{\alpha U_0}$$

$$\sum_{k=0}^{2m-1}(-1)^{k+1}t_k + \sum_{k=2m}^{2m+2n-1}(-1)^k t_k = 0$$

$$\sum_{k=0}^{2m-1}(-1)^k\exp(\zeta\omega t_k)\cos(\omega_d t_k) + \sum_{k=2m}^{2m+2n-1}(-1)^{k+1}\exp(\zeta\omega t_k)\cos(\omega_d t_k) = 0$$

$$\sum_{k=0}^{2m-1}(-1)^k\exp(\zeta\omega t_k)\sin(\omega_d t_k) + \sum_{k=2m}^{2m+2n-1}(-1)^{k+1}\exp(\zeta\omega t_k)\sin(\omega_d t_k) = 0$$

$$U_0\sum_{k=0}^{2m+2n-2}(-1)^k t_{k+1} = S \tag{24}$$

The optimal switching and maneuver times shown in Fig. 2 correspond to case I profiles with three sign reversals ($m = 3$) and case II profiles with two positive pulses followed by two negative pulses ($m = 2$, $n = 2$). In Fig. 2, after $S = 20.4$, the control profiles become time-optimal commands without fuel constraints, and $t_2 = t_1$, $t_4 = t_3$, $t_6 = t_5$, and thus become bang–bang commands rather than commands with coast periods. We also remark that case I profiles are more prevalent when the amount of fuel S is relatively close to the amount required by a typical time-optimal bang–bang without fuel constraint. Case II profiles tend to occur as optimal commands when the amount of fuel is relatively low compared to that of case I.

We observe that the specified fuel formulation of the time-optimal problem allows appreciable savings in fuel expenditure while incurring only a small penalty in maneuver time, especially in case I profiles. For example, in Fig. 2a, a 22% decrease in fuel (S goes from 20.4 to 16) incurs a 0.6% increase in maneuver time (t_f goes from 20.4 to 20.52).

In Refs. 12 and 13, case I and case II profiles are referred to as nonfuel-efficient and fuel-efficient profiles, respectively, due to the amount of fuel required to perform a prescribed maneuver. The profiles discussed in Refs. 12 and 13 are largely motivated by command shaping techniques that are efficient in terms of fuel expenditure, and the development of these profiles is based on intuitive ideas that modify typical time-optimal commands (without fuel constraints) by introducing coast periods at various places during the

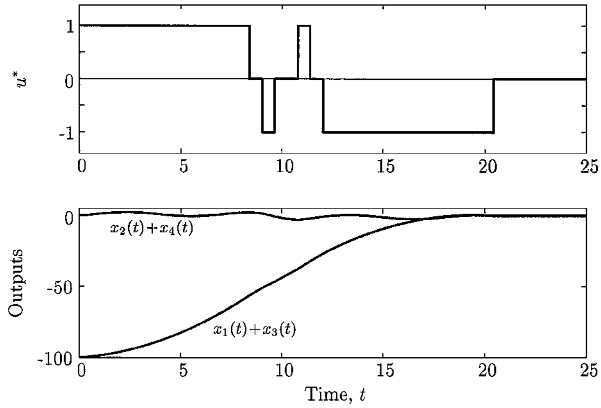

Fig. 3 Optimal control u^* and time response: $\omega_{\text{model}} = 1$, $\zeta_{\text{model}} = 0$, $L = 100$, and $S = 18$.

control action. For obvious reasons, fuel-efficient profiles are favored in Refs. 12 and 13. However, in the present work we have provided a mathematical justification for the existence of both types of profiles and emphasize that savings in fuel is still viable in case I profiles while achieving near-optimal maneuver times.

Figure 3 shows typical control and state time histories. In the example trajectory in Fig. 3, the position is slewed a distance of $L = 100$ such that the actuator and fuel limits are not exceeded. After the end of the maneuver, there is no residual vibration if the system model is accurate.

The parameter optimization problems formulated in Eq. (20) or Eq. (24), where the parameter t_f is to be minimized, will provide solutions that meet the necessary conditions imposed by the boundary constraints. However, these nonlinear parameter optimization problems are susceptible to local minima. A procedure for testing the optimality of solutions may be found in Ref. 13.

Properties of Commands for Flexible Structures

In this section, we explore some properties of optimal commands for rest-to-rest maneuvers of undamped flexible structures. We consider the following lumped parameter model for a flexible structure with multiple flexible modes and a single actuator:

$$\dot{\tilde{x}}(t) = \begin{bmatrix} 0 & 1 & & & & & & & \\ 0 & 0 & & & & & & & \\ & & 0 & 1 & & & & & \\ & & -\omega_1^2 & 0 & & & & & \\ & & & & 0 & 1 & & & \\ & & & & -\omega_2^2 & 0 & & & \\ & & & & & & \ddots & & \\ & & & & & & & 0 & 1 \\ & & & & & & & -\omega_r^2 & 0 \end{bmatrix} \tilde{x}(t) + \begin{bmatrix} 0 \\ 1 \\ 0 \\ b_1 \\ 0 \\ b_2 \\ \vdots \\ 0 \\ b_r \end{bmatrix} u(t) \tag{25}$$

with boundary conditions

$$\tilde{x}(0) = [-L \quad 0 \quad \cdots \quad 0 \quad 0]^T$$

$$\tilde{x}(t_f) = [0 \quad 0 \quad \cdots \quad 0 \quad 0]^T \tag{26}$$

where r is the number of flexible modes and t_f is the maneuver time. In addition, we have the bounded control and specified fuel constraints given by

$$|u(t)| \le U_0, \qquad t \in [0, t_f] \tag{27}$$

$$\int_0^{t_f} |u(t)| \, \mathrm{d}t = S \tag{28}$$

respectively. Let us define a new variable z as

$$z(t) = \int_0^t |u(\tau)| \, \mathrm{d}\tau - S$$

so that

$$\dot{z}(t) = |u(t)| \tag{29}$$

If we aggregate the preceding equations in the variable z to the original model (25) and (26), then the rest-to-rest motion of the flexible structure with specified fuel is described by the following augmented model:

$$\dot{x}(t) = \begin{bmatrix} 0 & 1 & & & & & & & & \\ 0 & 0 & & & & & & & & \\ & & 0 & 1 & & & & & & \\ & & -\omega_1^2 & 0 & & & & & & \\ & & & & 0 & 1 & & & & \\ & & & & -\omega_2^2 & 0 & & & & \\ & & & & & & \ddots & & & \\ & & & & & & & 0 & 1 & \\ & & & & & & & -\omega_r^2 & 0 & \\ 0 & 0 & & & \cdots & & & 0 & 0 & \end{bmatrix} x(t) + \begin{bmatrix} 0 \\ 1 \\ 0 \\ b_1 \\ 0 \\ b_2 \\ \vdots \\ 0 \\ b_r \\ \mathrm{sgn}[u(t)] \end{bmatrix} u(t) \tag{30}$$

where $x = [\tilde{x} \;\; z]^T$ is the augmented state vector, along with the boundary conditions

$$x(0) = [-L \quad 0 \quad \cdots \quad 0 \quad -S]^T$$

$$x(t_f) = [0 \quad 0 \quad \cdots \quad 0 \quad 0]^T \tag{31}$$

and subject to the constraint in Eq. (27).

A few properties of the time-optimal control of undamped flexible structures as in Eq. (25) have been outlined and proven in Refs. 4–6 when there are no fuel constraints. Here, we demonstrate that similar properties hold even in the presence of the fuel constraint.

Theorem 1: The time-optimal control $u^*(t), t \in [0, t_f^*]$, that drives the system (30) while satisfying (27) and (31) is antisymmetric about the midmaneuver time $t_f^*/2$, that is,

$$u^*(t) = -u^*\left(t_f^* - t\right) \tag{32}$$

Proof of Theorem 1: This proof is an extension of the one provided in Ref. 4. Here we additionally account for fuel constraints. Let us define $\tau = t_f^* - t$. Hence,

$$-\frac{\mathrm{d}}{\mathrm{d}\tau} x(\tau) = \frac{\mathrm{d}}{\mathrm{d}t} x(t)$$

and if we denote $(\mathrm{d}/\mathrm{d}\tau)[\cdot] = [\cdot]'$, Eq. (30) becomes

$$x_1'(\tau) = -x_2(\tau), \qquad x_2'(\tau) = -u(\tau)$$

$$x_3'^k(\tau) = -x_4^k(\tau), \qquad k = 1, \ldots, r$$

$$x_4'^k(\tau) = \omega_k^2 x_3^k(\tau) - b_k u(\tau), \qquad k = 1, \ldots, r$$

$$z'(\tau) = -|u(\tau)| \tag{33}$$

We have reformulated the original problem in terms of the new independent variable τ. The problem now consists of finding the optimal control $u(\tau)$ bounded by Eq. (27), $\tau \in [0, \tau_f]$, that drives Eq. (33) and satisfies the boundary conditions

$$x(\tau)|_{\tau=0} = [0 \quad 0 \quad \cdots \quad 0 \quad 0]^T$$
$$x(\tau)|_{\tau=\tau_f} = [-L \quad 0 \quad \cdots \quad 0 \quad -S]^T \tag{34}$$

Let $\hat{u}(\tau)$, $\tau \in [0, \hat{\tau}_f]$, be the optimal control for Eqs. (33) and (34), where $\hat{\tau}_f$ denotes the minimum value attained by τ_f. Because Eqs. (30) and (31) and (33) and (34) constitute the same problem, we clearly have

$$\hat{\tau}_f = t_f^*, \qquad \hat{u}[\tau(t)] = u^*(t) \tag{35}$$

If we make the change of variables in our original problem

$$\hat{x}(t) = x(t) + [L \quad 0 \quad \cdots \quad 0 \quad S]^T$$

the boundary conditions in Eq. (31) become those of Eq. (34) with opposite sign, that is,

$$\hat{x}(0) = [0 \quad 0 \quad \cdots \quad 0 \quad 0]^T, \qquad \hat{x}(t_f) = [L \quad 0 \quad \cdots \quad 0 \quad S]^T \tag{36}$$

Because Eq. (30) is still the governing equation for the newly defined state vector $\hat{x}$, the time-optimal solution to this problem remains $u^*(t)$, $t \in [0, t_f^*]$, along with Eq. (27).

Comparing Eq. (30), with x replaced by $\hat{x}$, and Eq. (33), we observe that they are essentially the same governing equations in the independent variables t and τ, respectively, with zero initial conditions but with opposite signs for the terminal conditions [compare Eqs. (36) and (34)]. By linearity, we conclude that the optimal controls $\hat{u}(\cdot)$ and $u^*(\cdot)$ have the same magnitude with opposite signs, that is,

$$\hat{u}[\tau(t)] = -u^*[\tau(t)]$$

and by Eq. (35)

$$u^*(t) = -u^*[\tau(t)] = -u^*\left(t_f^* - t\right) \tag{37}$$

This proves the theorem.

Remark: From Theorem 1, two remarks follow:

1) The number of sign reversals m in Eq. (17) must be an odd number for case I profiles.

2) The number of pulses m and n in Eq. (21) must be equal for case II profiles.

We will use these remarks and the symmetry property stated in Theorem 1 to establish the following result.

Lemma: For an undamped one-mode flexible system, of form (15) with $\zeta = 0$, with boundary conditions $x(0) = [-L \ 0 \ 0 \ 0]^T$ and $x(t_f) = \mathbf{0}$, the state at the midmaneuver time $t_f/2$ is given by

$$x(t_f/2) = [-L/2 \quad x_2(t_f/2) \quad 0 \quad x_4(t_f/2)]^T \tag{38}$$

where $x_2(t_f/2)$ and $x_4(t_f/2)$ are any real numbers, provided that the driving control (17) [or Eq. (21)] satisfies the symmetry property of Theorem 1. In addition, the fuel state z at midmaneuver is $z(t_f/2) = -S/2$, where the boundary conditions are $z(0) = -S$ and $z(t_f) = 0$, provided that the control satisfies the symmetry property of Theorem 1.

Proof of Lemma: We only outline the proof that corresponds to case I, that is, control given by Eq. (17), and omit the detailed algebraic manipulations.

We can use Eqs. (18) to compute the state at time $t = t_f/2$. Although Eqs. (18) were written for $t \geq t_f$, these equations are still valid for $t < t_f$ if we consider the pulses of the control that are relevant in the analysis. For the rigid body, at $t = t_f/2$,

$$x_2\left(\frac{t_f}{2}\right) = \alpha U_0 \sum_{k=0}^{[m/2]} \left[(-1)^k\left(\frac{t_f}{2} - t_{2k}\right) + (-1)^{k+1}\left(\frac{t_f}{2} - t_{2k+1}\right)\right]$$

which can be any real number, where the notation $[m/2]$ denotes the largest integer less than or equal to $m/2$. Also,

$$x_1(t_f) = -L + \alpha U_0 \sum_{k=0}^{[m/2]} \left[(-1)^k\left(\frac{t_f}{2} - t_{2k}\right)^2 + (-1)^{k+1}\left(\frac{t_f}{2} - t_{2k+1}\right)^2\right] = 0$$

implies that

$$x_1\left(\frac{t_f}{2}\right) = -L + \frac{\alpha U_0}{2} \sum_{k=0}^{[m/2]} \left[(-1)^k\left(\frac{t_f}{2} - t_{2k}\right)^2 + (-1)^{k+1}\left(\frac{t_f}{2} - t_{2k+1}\right)^2\right] = -\frac{L}{2}$$

For the flexible mode, we have that

$$x_3(t_f) = -2\cos\left(\omega\frac{t_f}{2}\right)\frac{\alpha b_1 U_0}{\omega^2} \sum_{k=0}^{[m/2]} \left\{(-1)^k \cos\left[\omega\left(\frac{t_f}{2} - t_{2k}\right)\right] + (-1)^{k+1}\cos\left[\omega\left(\frac{t_f}{2} - t_{2k+1}\right)\right]\right\} = 0$$

and, hence,

$$x_3\left(\frac{t_f}{2}\right) = -\frac{\alpha b_1 U_0}{\omega^2} \sum_{k=0}^{[m/2]} \left\{(-1)^k \cos\left[\omega\left(\frac{t_f}{2} - t_{2k}\right)\right] + (-1)^{k+1}\cos\left[\omega\left(\frac{t_f}{2} - t_{2k+1}\right)\right]\right\} = 0$$

$$x_4\left(\frac{t_f}{2}\right) = \frac{\alpha b_1 U_0}{\omega} \sum_{k=0}^{[m/2]} \left\{(-1)^k \sin\left[\omega\left(\frac{t_f}{2} - t_{2k}\right)\right] + (-1)^{k+1}\sin\left[\omega\left(\frac{t_f}{2} - t_{2k+1}\right)\right]\right\}$$

can be any real number.

Note that the fuel state at midmaneuver time, $z(t_f/2) = -S/2$, follows readily from the symmetry property of Theorem 1.

Theorem 2: For the specified fuel, time-optimal control of Eqs. (30) and (31), along with Eq. (27), the numerical value of the multiplier corresponding to the fuel state p_z is equal to the augmented switching function $\sigma(t)$ evaluated at $t = t_f^*/2$, that is,

$$\sigma\left(t_f^*/2\right) = \pm p_z \tag{39}$$

where

$$\sigma(t) = \boldsymbol{p}^T(t)\boldsymbol{b} \pm p_z$$

and t_f^* is the optimal maneuver time.

Proof of Theorem 2: This is an extension of the proof in Ref. 11 to the case with fuel constraint. From the lemma, the rigid-body position and the kth flexible mode position at midmaneuver time $t_f^*/2$ are

$$x_1\left(t_f^*/2\right) = -L/2, \qquad x_3^k\left(t_f^*/2\right) = 0, \qquad k = 1, \ldots, r$$

respectively.

Now consider the optimal control problem

$$\text{minimize} \int_0^{t_f/2} \mathrm{d}t \quad \text{or minimize} \quad \frac{t_f}{2}$$

with boundary conditions

$$\boldsymbol{x}(0) = [-L \quad 0 \quad 0 \quad \cdots \quad 0 \quad 0 \quad -S]^T, \qquad \boldsymbol{x}(t_f/2) = \left[-L/2 \quad x_2(t_f/2) \quad 0 \quad x_4^1(t_f/2) \quad 0 \quad x_4^2(t_f/2) \quad \cdots \quad 0 \quad x_4^r(t_f/2) \quad -S/2\right]^T$$

Because the position states $x_1(t_f/2)$ and $x_3^k(t_f/2)$ are fixed, the velocity states $x_2(t_f/2)$ and $x_4^k(t_f/2)$ are free, and the fuel state $z(t_f/2)$ is fixed, the transversality condition requires that the costate vector be of the form

$$\left[\boldsymbol{p}^T(t_f/2) \quad p_z\right] = \left[p_1(t_f/2) \quad 0 \quad p_3^1(t_f/2) \quad 0 \quad p_3^2(t_f/2) \quad 0 \quad \cdots \quad p_3^r(t_f/2) \quad 0 \quad p_z\right]$$

Then the switching function for the augmented system evaluated at midmaneuver time is

$$\sigma\left(\frac{t_f^*}{2}\right) = \boldsymbol{p}^T\left(\frac{t_f^*}{2}\right)\boldsymbol{b} \pm p_z =$$

$$\left[p_1\left(\frac{t_f^*}{2}\right) \quad 0 \quad p_3^1\left(\frac{t_f^*}{2}\right) \quad 0 \quad p_3^2\left(\frac{t_f^*}{2}\right) \quad 0 \quad \cdots \quad p_3^r\left(\frac{t_f^*}{2}\right) \quad 0\right]$$

$$\times \begin{bmatrix} 0 \\ 1 \\ 0 \\ b_1 \\ 0 \\ b_2 \\ \vdots \\ 0 \\ b_r \end{bmatrix} \pm p_z = \pm p_z$$

and the result follows.

Remark: In a typical time-optimal problem (without fuel constraint), the optimal control is bang–bang and the symmetry property implies that $t = t_f^*/2$ is a switching time and, hence, $p_z = 0$ because $\sigma(t_f^*/2) = 0$. If the specified fuel S is less than the amount of fuel required by a typical time-optimal maneuver, then $p_z \neq 0$, as it should be because $t_f^*/2$ is not a switching time, because the optimal control now is of the bang–off-bang type with $t_f^*/2$ located at the center of one of the off periods.

Robustness of Commands

In this section we investigate robustness issues concerning time-optimal commands with specified fuel. The time-optimal commands derived from the solutions of the optimization problems (20) or (24) will meet the desired boundary constraints for a given set of modeled parameters, for example, $\omega = \omega_0$ and $\zeta = \zeta_0$. It is also clear that at the end of the maneuver the same boundary constraints cannot be met with the same control when there is a slight variation in the modeled parameters as shown in Fig. 4.

For a range about the modeling parameters, the optimal commands tend to be slightly more robust when the amount of fuel is decreased, as one can infer from examination of the levels of the weighted residual energy of the modal states (Fig. 5), where the weighted residual energy is determined as[6]

$$E_r = \frac{1}{2}\sum_{i=1}^{r}\omega_i^2\left[\left(x_3^i\right)^2 + \left(x_4^i\right)^2\right] \tag{40}$$

evaluated at $t = t_f$. Because reducing fuel consumption only increases robustness a small amount and also causes the move time t_f to be increased slightly, it is desirable to have a design procedure for deriving time-optimal commands that are robust to parameter variations and yet use a fixed amount of fuel. We also note that optimal commands are less sensitive to variations in damping than they are to variations in frequency (compare levels of weighted residual energy in Figs. 5a and 5b).

Similar to the procedure suggested in Refs. 7, 8, and 14, one way to obtain more robust designs is to set the derivatives of the modal states with respect to the modeling parameters equal to zero at the end of the maneuver, that is,

$$\left.\frac{\partial x_3}{\partial \omega}\right|_{t=t_f} = 0, \qquad \left.\frac{\partial x_4}{\partial \omega}\right|_{t=t_f} = 0 \tag{41}$$

or

$$\left.\frac{\partial x_3}{\partial \zeta}\right|_{t=t_f} = 0, \qquad \left.\frac{\partial x_4}{\partial \zeta}\right|_{t=t_f} = 0 \tag{42}$$

and use the resulting equations as additional constraints in Eqs. (20) and (24). Note that Eqs. (41) and (42) lead to the same constraint equations, and hence, robustness with respect to variations in ω will also lead to robustness with respect to variations in ζ. Therefore, robust time-optimal commands can be derived from the solutions of the following constrained optimization problems.

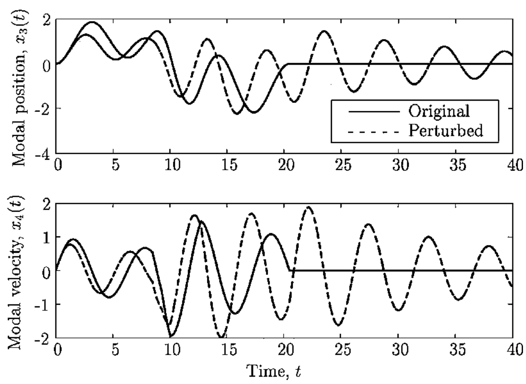

Fig. 4 Modal states under parameter variations; original system designed for $\omega_{model} = 1$, $\zeta_{model} = 0.05$, $L = 100$, and $S = 17$. The perturbed response is the result of parameter variations; here, $\omega_{actual} = 1.2$.

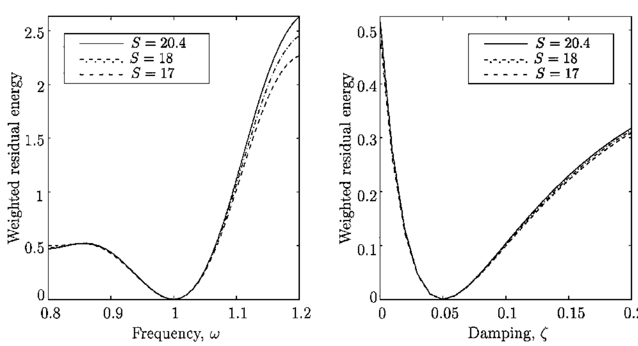

a) Variations in frequency **b) Variations in damping**

Fig. 5 Sensitivity to parameter variations where modeled parameters are $\omega_{model} = 1$, $\zeta_{model} = 0.05$, and $L = 100$.

Case I

Minimize t_f subject to

$$\sum_{k=0}^{m}\left[(-1)^k t_{2k}^2 + (-1)^{k+1} t_{2k+1}^2\right] = \frac{2L}{\alpha U_0}$$

$$\sum_{k=0}^{m}\left[(-1)^{k+1} t_{2k} + (-1)^k t_{2k+1}\right] = 0$$

$$\sum_{k=0}^{m}\Big[(-1)^k \exp(\zeta\omega t_{2k})\cos(\omega_d t_{2k}) + (-1)^{k+1}\exp(\zeta\omega t_{2k+1})\cos(\omega_d t_{2k+1})\Big] = 0$$

$$\sum_{k=0}^{m}\Big[(-1)^k \exp(\zeta\omega t_{2k})\sin(\omega_d t_{2k}) + (-1)^{k+1}\exp(\zeta\omega t_{2k+1})\sin(\omega_d t_{2k+1})\Big] = 0$$

$$\sum_{k=0}^{m}\Big[(-1)^k t_{2k}\exp(\zeta\omega t_{2k})\cos(\omega_d t_{2k}) + (-1)^{k+1} t_{2k+1}\exp(\zeta\omega t_{2k+1})\cos(\omega_d t_{2k+1})\Big] = 0$$

$$\sum_{k=0}^{m}\Big[(-1)^k t_{2k}\exp(\zeta\omega t_{2k})\sin(\omega_d t_{2k}) + (-1)^{k+1} t_{2k+1}\exp(\zeta\omega t_{2k+1})\sin(\omega_d t_{2k+1})\Big] = 0$$

$$U_0\sum_{k=0}^{2m}(-1)^k t_{k+1} = S \tag{43}$$

Case II

Minimize t_f subject to

$$\sum_{k=0}^{2m-1}(-1)^k t_k^2 + \sum_{k=2m}^{2m+2n-1}(-1)^{k+1} t_k^2 = \frac{2L}{\alpha U_0}$$

$$\sum_{k=0}^{2m-1}(-1)^{k+1} t_k + \sum_{k=2m}^{2m+2n-1}(-1)^k t_k = 0$$

$$\sum_{k=0}^{2m-1}(-1)^k \exp(\zeta\omega t_k)\cos(\omega_d t_k) + \sum_{k=2m}^{2m+2n-1}(-1)^{k+1}\exp(\zeta\omega t_k)\cos(\omega_d t_k) = 0$$

$$\sum_{k=0}^{2m-1}(-1)^k \exp(\zeta\omega t_k)\sin(\omega_d t_k) + \sum_{k=2m}^{2m+2n-1}(-1)^{k+1}\exp(\zeta\omega t_k)\sin(\omega_d t_k) = 0$$

$$\sum_{k=0}^{2m-1}(-1)^k t_k\exp(\zeta\omega t_k)\cos(\omega_d t_k) + \sum_{k=2m}^{2m+2n-1}(-1)^{k+1} t_k\exp(\zeta\omega t_k)\cos(\omega_d t_k) = 0$$

$$\sum_{k=0}^{2m-1}(-1)^k t_k\exp(\zeta\omega t_k)\sin(\omega_d t_k) + \sum_{k=2m}^{2m+2n-1}(-1)^{k+1} t_k\exp(\zeta\omega t_k)\sin(\omega_d t_k) = 0$$

$$U_0\sum_{k=0}^{2m+2n-2}(-1)^k t_{k+1} = S \tag{44}$$

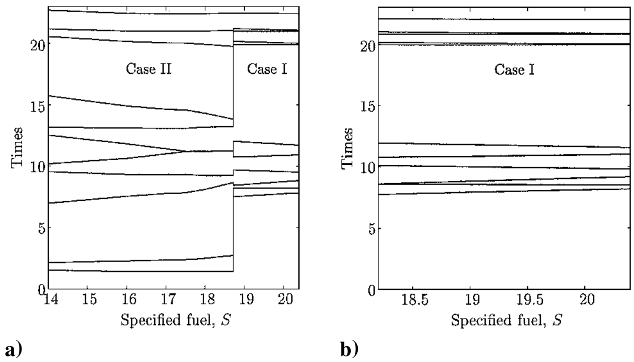

Fig. 6 Switching and maneuver times as a function of specified fuel for robust designs: a) $\omega_{\text{model}} = 1$, $\zeta_{\text{model}} = 0$, and $L = 100$ and b) $\omega_{\text{model}} = 1$, $\zeta_{\text{model}} = 0.05$, and $L = 100$.

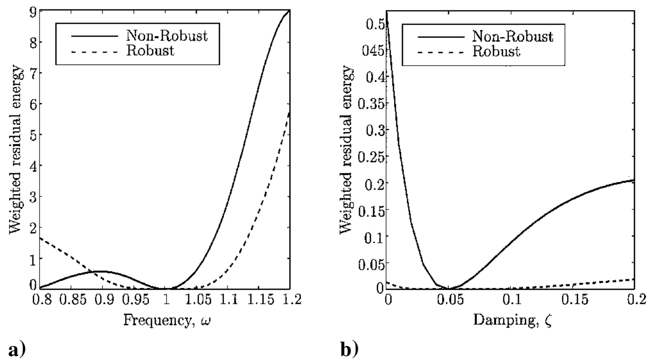

Fig. 7 Sensitivity of robust time-optimal designs to parameter variations: a) variations in frequency when $\omega_{\text{model}} = 1$, $\zeta_{\text{model}} = 0$, $L = 100$, and $S = 20$ and b) variations in damping when $\omega_{\text{model}} = 1$, $\zeta_{\text{model}} = 0.05$, $L = 100$, and $S = 20$.

Figure 6 shows the robust time-optimal designs. In comparison with the results in Fig. 2, we note that the robust designs involve more switching times and incur a penalty in terms of maneuver times for the range of fuel considered. For instance, in Fig. 6 the maneuver times are approximately 9% longer than the non robust maneuver times of Fig. 2, for example, t_f increases from 20.52 to 22.46 for $S = 16$. As mentioned before, case II profiles are optimal when the amount of fuel S is relatively low compared to that of case I profiles (as shown in Fig. 6a). Beyond a certain S, these robust designs become bang–bang commands without coast periods.

We also remark that for undamped systems, the robust time-optimal designs are not necessarily antisymmetric (see case I in Fig. 6). In some instances, if the proper multipliers are zero, the control profiles may be antisymmetric (see case II in Fig. 6), but this is not the case in general. This can be explicated from the constraints in Eqs. (43) or (44). These equations would correspond to the time-optimal problem of a fictitious system with double poles at the same location of the poles of the original system (15) (Ref. 8). As a consequence, the costate equation will include terms of the form $t\exp(\zeta\omega t)\cos(\omega_d t)$ and $t\exp(\zeta\omega t)\sin(\omega_d t)$ due to the repeated poles (eigenvalues). The presence of these terms in the costate equation reveals that the intersection of the switching curve with the horizontal lines at $\pm p_z$ may not occur at places that lead to antisymmetric profiles for undamped systems.

The sensitivities of these robust designs are presented in Fig. 7. In general, robust designs improve insensitivity to parameter variations about modeled parameters, but may lead to larger errors if the actual parameters are far from the modeled ones (Fig. 7a).

Conclusions

We have provided a mathematical justification for time-optimal commands with specified fuel and applied this knowledge to the control of flexible structures. Open-loop time-optimal controls subject to fuel constraints were obtained by solving a parameter optimization problem. Symmetry properties of the optimal commands for undamped flexible structures were established. We have also observed that time-optimal designs with fuel constraints are more sensitive to frequency variations than they are to damping variations, and the sensitivity to parameter variations is reduced as the amount of fuel is decreased. A robust time-optimal design procedure has been discussed to utilize the total fuel at our disposal. These robust time-optimal controls lead to better designs with a small penalty in terms of maneuver times, but do not satisfy symmetry properties even when there is no damping.

Acknowledgments

The authors gratefully acknowledge support from a National Science Foundation Early Faculty CAREER Award (Grant CMS-9625086), the Colorado Advanced Software Institute, Storage Technology Corporation, and an Office of Naval Research Young Investigator Award (Grant N00014-97-1-0642).

References

[1]Book, W. J., "Controlled Motion in an Elastic World," *Journal of Dynamic Systems, Measurement, and Control*, Vol. 115, No. 2, 1993, pp. 252–261.

[2]Junkins, J. L., and Kim, Y., *Introduction to Dynamics and Control of Flexible Structures*, AIAA Education Series, AIAA, Washington, DC, 1993.

[3]Kirk, D. E., *Optimal Control Theory: An Introduction,* Prentice–Hall, Upper Saddle River, NJ, 1970.

[4]Ben-Asher, J., Burns, J. A., and Cliff, E. M., "Time-Optimal Slewing of Flexible Spacecraft," *Journal of Guidance, Control, and Dynamics*, Vol. 15, No. 2, 1992, pp. 360–367.

[5]Pao, L. Y., and Franklin, G. F., "Time-Optimal Control of Flexible Structures," *Proceedings of the 29th Conference on Decision and Control*, Inst. of Electrical and Electronics Engineers, New York, 1990, pp. 2580, 2581.

[6]Singh, G., Kabamba, P. T., and McClamroch, N. H., "Planar, Time-Optimal, Rest-to-Rest Slewing Maneuvers of Flexible Spacecraft," *Journal of Guidance, Control, and Dynamics*, Vol. 12, No. 1, 1989, pp. 71–81.

[7]Liu, Q., and Wie, B., "Robust Time-Optimal Control of Uncertain Flexible Spacecraft," *Journal of Guidance, Control, and Dynamics*, Vol. 15, No. 3, 1992, pp. 597–604.

[8]Pao, L. Y., and Singhose, W. E., "Robust Minimum Time Control of Flexible Structures," *Automatica*, Vol. 34, No. 2, 1998, pp. 229–236.

[9]Pao, L. Y., "Minimum-Time Control Characteristics of Flexible Structures," *Journal of Guidance, Control, and Dynamics*, Vol. 19, No. 1, 1996, pp. 123–129.

[10]Singh, T., "Effect of Damping on the Structure of the Time-Optimal Control Profile," *Journal of Guidance, Control, and Dynamics*, Vol. 19, No. 5, 1996, pp. 1182–1184.

[11]Singh, T., "Fuel/Time Optimal Control of the Benchmark Problem," *Journal of Guidance, Control, and Dynamics*, Vol. 18, No. 6, 1995, pp. 1225–1231.

[12]Singhose, W., Bohlke, K., and Seering, W., "Fuel-Efficient Pulse Command Profiles for Flexible Spacecraft," *Journal of Guidance, Control, and Dynamics*, Vol. 19, No. 4, 1996, pp. 954–960.

[13]Singhose, W., Singh, T., and Seering, W., "On-Off Control with Specified Fuel Usage," *Journal of Dynamic Systems, Measurement, and Control*, Vol. 121, No. 2, 1999, pp. 206–212.

[14]Liu, S., and Singh, T., "Robust Time-Optimal Control of Flexible Structures with Parameter Uncertainty," *Journal of Dynamic Systems, Measurement, and Control*, Vol. 119, No. 4, 1997, pp. 743–748.